Interrelationship between Mg/Fe Ratio and Octahedral Al Content in Biotite

Charles V. Guidotti, John T. Cheney,

Department of Geology and Geophysics, University of Wisconsin, Madison, Wisconsin 53706

and Paul D. Conatore

Department of Geology, Colorado School of Mines, Golden, Colorado 80401

Abstract

The trend of a plot by Foster (1960) of Mg *vs* (Fe^{2+} + Mn) *vs* R^{3+} (Al, Ti, Fe^{3+}) in the octahedral sheet of biotite has led some workers to infer an inverse correlation between Al^{VI} and Mg/Fe^{2+} ratio. This paper presents arguments and data which indicate that such a correlation does not exist over most of the biotite composition range and that the trend mentioned above is in part an accident of sample availability.

Introduction

Foster (1960) made a very useful and comprehensive survey of the compositional range of the trioctahedral micas that are broadly designated as biotites. Included were compositions encompassed by the end members phlogopite, $KMg_3(AlSi_3O_{10})(OH)_2$; eastonite, $K(Mg_{2.5}Al_{0.5})(Al_{1.5}Si_{2.5}O_{10})(OH)_2$; annite, $KFe_3(AlSi_3O_{10}(OH)_2$; and siderophyllite, $K(Fe_{2.5}Al_{0.5})$ $(Al_{1.5}Si_{2.5}O_{10})(OH)_2$. In this note "biotite" refers to micas plotting within the field bounded by these four end members.

Based upon a compilation of a large number of analyses from many different parageneses, Foster (1960, Fig. 11; Fig. 1, this paper) made an interesting triangular plot of Mg *vs* (Fe^{2+} + Mn) *vs* R^{3+} (includes Al, Ti^{4+}, Fe^{3+}) in the octahedral sheet of biotite. The points lie in a distinct band (Fig. 1) in which Al^{VI} appears to decrease with increase of $Mg/(Fe^{2+}$ + Mn). However, in discussing this band, Foster (1960, p. 25) states, "The trioctahedral micas may, therefore, be thought of as members of a system characterized by concurrent but independent replacement of Mg by Fe^{2+} and R^{3+} ions." Nonetheless, because of the shape and orientation of the band shown in Figure 1, several workers have inferred that changes in the Mg *vs* (Fe^{2+} + Mn) content of the octahedral sheet control the amount of Al^{VI}. For example, such a relationship has been tacitly implied by Hazen and Wones (1972, p. 124) when they state,

"As the Fe^{2+} content of these micas increases, so does the octahedral aluminum content." Gower (1957) constructed a diagram quite similar to that of Foster (1960) using data from specimens of diverse origin. He also inferred (p. 155) "A greater tolerance for octahedral aluminum is indicated in iron-rich varieties."

The goal of this paper is to demonstrate that, with the possible exception of biotites very near the annite-siderophyllite join, no clear relationship exists between the $Mg/(Fe^{2+}$ + Mn) ratio and octahedral Al content. Hence, any inferences of a direct relationship between these two factors should be reconsidered. Moreover, it will be shown that the specific, detailed pattern shown on Figure 1 (or on Gower's Fig. 5) is in part an accident.

Our approach is largely empirical, inasmuch as little attention is given to the substitutional models applicable to the octahedral and tetrahedral sheets of trioctahedral micas. We have followed the common practice of assigning Mg, Fe^{2+}, Ti, and Al in excess of that needed to fill tetrahedral sites to the octahedral sheet.

Discussion of the Band of Points on Figure 1

Several factors appear to explain the orientation of the band of points shown on Figure 1.

The tapering of the biotite field toward the
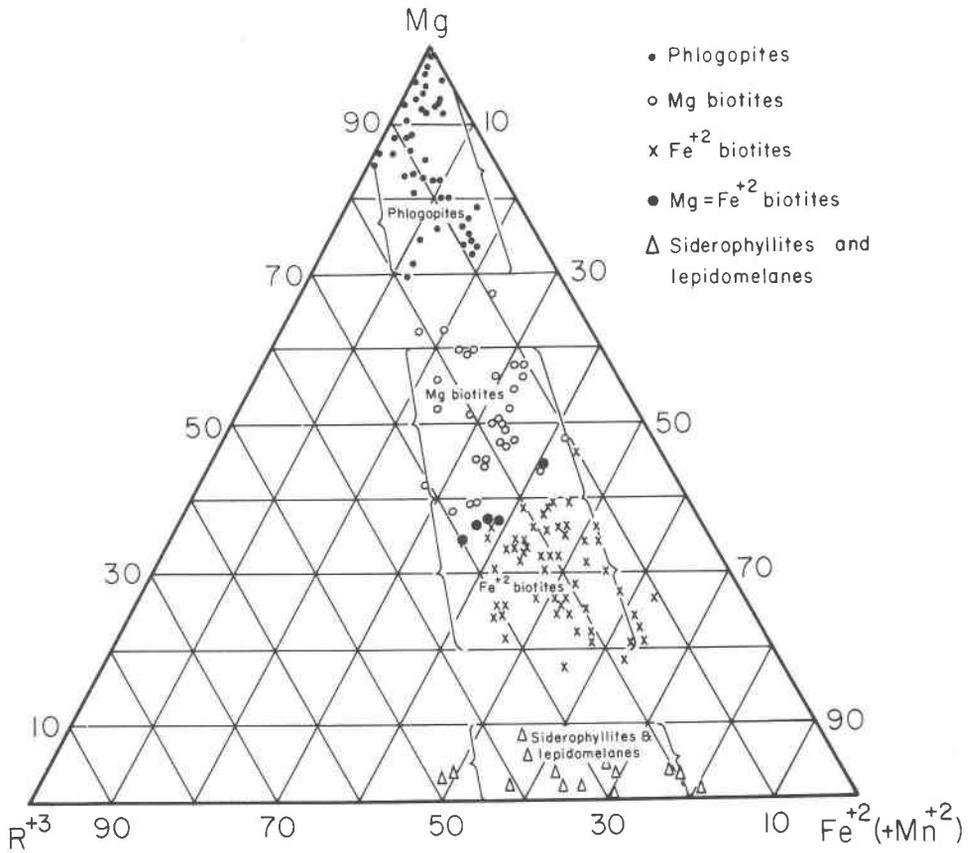
FIG. 1. Plot of octahedral $R^{3+}(=Al + Fe^{3+} + Ti)$ *vs* Mg *vs* $(Fe^{2+} + Mn)$ in more than 200 natural biotites from various parageneses. Diagram based on Foster (1960, Fig. 11).
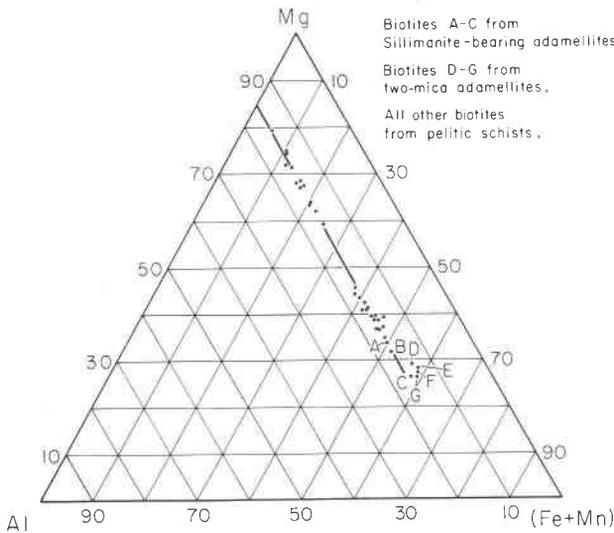
FIG. 2. Plot of octahedral Al *vs* Mg *vs* $(Fe^{2+} + Mn)$ in biotites from northwestern Maine. Biotites A, B, and C from sillimanite-bearing adamellite; biotites D, E, F, and G from two-mica adamellite (see Table 1E). All other biotites from pelitic schists with sillimanite, staurolite, or cordierite (see Tables 1–4). Best fit line is visually located.
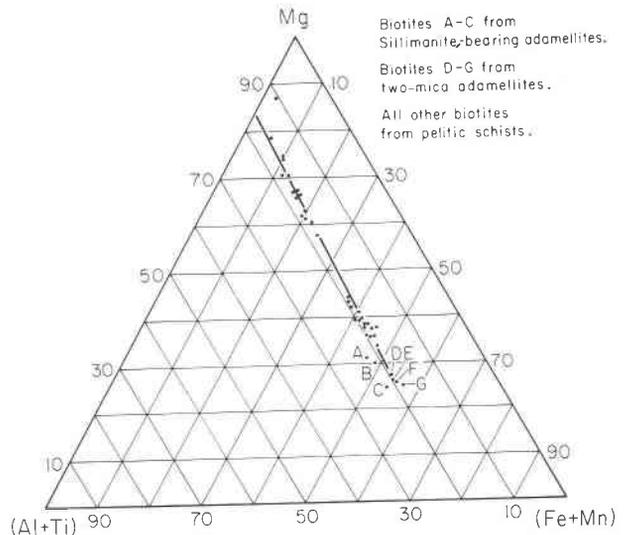
FIG. 3. Plot of octahedral (Al + Ti) *vs* Mg *vs* $(Fe^{2+} + Mn)$ in the same biotites as on Figure 2. Best fit line is visually located.

TABLE 1. Analyses of Biotites from Staurolite and/or Sillimanite Bearing Rocks from the Staurolite to Lower Sillimanite Zones of the Rangeley Quadrangle, Maine*

Wt%		57	42	27	30	77	123	104	119	109	201	247	231
SiO_2		34.95	35.39	35.60	35.79	35.74	35.94	34.92	36.12	35.42	35.50	34.88	35.31
Al_2O_3		19.48	19.80	19.94	20.06	20.15	20.01	19.98	19.95	20.22	20.27	20.03	20.10
FeO		20.80	19.57	20.72	19.04	19.82	18.60	21.58	20.23	19.05	20.54	21.20	20.56
MgO		9.85	9.79	9.15	10.30	9.77	10.69	8.71	10.03	10.57	9.17	9.31	9.76
TiO_2		1.50	1.55	1.72	1.70	1.53	1.67	1.55	1.68	1.72	1.83	1.84	1.63
MnO		.05	.06	.06	.08	.07	.06	.08	.08	.10	.07	.09	.11
K_2O		8.24	8.43	8.44	8.42	8.16	8.38	8.14	8.33	8.47	8.56	8.48	8.47
Na_2O		.25	.23	.35	.34	.43	.31	.33	.35	.28	.33	.32	.26
CaO		.02	.01	.01	.01	.01	.01	.03	.01	.04	–	.01	.01
BaO		.03	.02	.03	.03	.03	.03	.03	.03	.03	.03	.03	.03
ZnO		.03	.05	.01	.03	.05	.01	.01	.03	–	.03	.03	.02
H_2O		4.81	5.11	3.98	4.21	4.25	4.28	4.65	3.11	4.10	3.63	3.77	3.73
						Formula	Based on 22	Oxygen					
IV	Si	5.32	5.38	5.38	5.36	5.38	5.38	5.32	5.38	5.38	5.34	5.28	5.32
	Al	2.68	2.62	2.62	2.64	2.62	2.62	2.68	2.62	2.62	2.66	2.72	2.68
VI	Al	.82	.92	.92	.90	.94	.92	.92	.88	1.00	.94	.86	.88
	Fe	2.66	2.48	2.62	2.38	2.50	2.32	2.76	2.52	2.42	2.58	2.68	2.58
	Mg	2.24	2.22	2.06	2.30	2.18	2.38	1.98	2.24	2.38	2.06	2.10	2.18
	Ti	.18	.18	.20	.20	.18	.18	.18	.18	.20	.20	.20	.18
	Mn	.006	.006	.008	.010	.008	.008	.010	.010	.012	.008	.012	.014
	Zn	.002	.004	.002	.002	.006	–	–	.004	–	.006	.006	.002
	Σ	5.908	5.81	5.81	5.792	5.814	5.808	5.85	5.834	6.012	5.794	5.858	5.836
XII	K	1.60	1.64	1.62	1.62	1.56	1.60	1.58	1.58	1.64	1.64	1.64	1.62
	Na	.08	.068	.10	.10	.12	.10	.10	.10	.08	.10	.10	.08
	Ca	.004	.002	–	.002	–	.002	.006	–	.006	–	.002	.002
	Ba	.002	.002	.002	.002	.002	.002	.002	.002	.002	.002	.002	.002
	Σ	1.685	1.712	1.722	1.724	1.682	1.704	1.688	1.682	1.728	1.742	1.744	1.704

*Data from Table 4 of Guidotti (1974). Value cited for H_2O is by difference from 100 percent.

phlogopite end-member appears to be due in part to the plotting of Mg-rich biotites from Al-poor rocks such as marbles, calc-silicate granulites, and ultramafics. The vast majority of analyzed, Mg-rich biotites reported in the literature are from such rocks.

TABLE 2. Analyses of Biotites from Sulfide-Rich Small's Falls Formation, North Central Rumford Quandrangle, Maine. Upper Staurolite to Lower Sillimanite Zone†

Wt%		Ru-e28a -66*	Ru-e28b' -66*	Ru-D24- 66**	Ru-e31- 66*	Ru-e26- 66*	Ru-e25- 66*	Ru-e32- 66*	Ru-G24- 66*
SiO_2		38.83	38.76	39.53	39.08	39.57	40.14	39.14	40.81
Al_2O_3		20.06	19.80	19.17	19.38	19.60	18.98	19.62	19.50
FeO		9.53	9.44	8.13	7.72	6.01	4.81	4.75	2.53
MgO		16.72	17.28	18.32	18.49	19.57	20.59	20.36	22.28
TiO_2		0.98	1.04	0.85	0.75	0.66	0.58	0.65	0.52
MnO		0.29	0.25	0.31	0.20	0.20	0.20	0.28	0.18
K_2O		7.93	8.15	8.13	8.05	8.00	8.37	8.12	8.60
Na_2O		0.22	0.21	0.20	0.21	0.23	0.24	0.22	0.23
CaO		.00	.00	.00	.00	.00	.00	.00	.00
BaO		nd	nd	nd	nd	nd	nd	nd	nd
ZnO		nd	nd	nd	nd	nd	nd	nd	nd
H_2O		5.39	5.02	5.34	6.08	6.11	5.82	6.37	5.40
				Formula	Based on 22	Oxygen			
IV	Si	5.583	5.560	5.648	5.617	5.634	5.710	5.568	5.681
	Al	2.417	2.440	2.352	2.383	2.366	2.290	2.432	2.319
VI	Al	0.982	.908	.877	.900	.924	.871	.859	.879
	Fe	1.146	1.133	.971	.928	.716	.569	.565	.294
	Mg	3.583	3.695	3.901	3.960	4.154	4.335	4.423	4.622
	Ti	.106	0.112	.091	.081	.070	.062	.069	.055
	Mn	.036	0.030	.037	.024	.024	.028	.033	.021
	Σ	5.853	5.878	5.877	5.893	5.892	5.861	5.949	5.871
XII	K	1.455	1.491	1.482	1.475	1.454	1.508	1.474	1.528
	Na	.063	.059	.055	.059	.062	.067	.061	.062
	Ca	.000	.000	.000	.000	.000	.000	.000	.000
	Σ	1.518	1.550	1.537	1.534	1.516	1.575	1.535	1.590

*Contain Cord + Chte + Bio + Musc + Qtz + Plag.
**Contains Chte + Bio + Musc + Qtz + Plag.

† Data from Guidotti et al (1975). Value cited for H_2O by difference from 100 percent.

In these rocks, biotite usually does not coexist with aluminous minerals. Hence, it tends to plot toward the phlogopite end of the phlogopite-eastonite series. Moreover, Figure 1 and Gower's diagram show considerable scatter in $R^{3+}/(Mg + Mn + Fe^{2+})$. This scatter results from plotting biotite analyses from specimens from a multitude of different parageneses and bulk compositions. It will become evident below that this has also contributed to obscuring the true relationship between Al^{VI} content and the $Mg/(Fe^{2+} + Mn)$ ratio.

Figure 1 includes Fe^{3+} and Ti^{4+} as part of the R^{3+} term. As a result, Fe biotites, siderophyllites, and lepidomelanes plot noticeably nearer the R^{3+} corner (cf Figs. 2 and 3). Moreover, analyses discussed below show that Mg-rich biotites are in fact low in Ti.

Hence, the trend shown by the band of points in Figure 1 is in part an accident due to the availability of samples, and in part a function of what has been included with R^{3+}. The trend resulting from the latter aspect is of course real, but it should not be interpreted as implying a marked interrelationship between Al^{VI} content and the $Mg/(Fe^{2+} + Mn)$ ratio.[1]

[1] It must be reemphasized that in biotites near the pure Fe end members such a relationship may exist. This is evident from the discussion of Hazen and Wones (1972). Our data do not bear directly on this composition range.

TABLE 3. Analyses of Biotites from Sulfide-Rich Small's Falls Formation, Southwest Rumford Quadrangle, Maine. Upper Sillimanite to K-Feldspar + Sillimanite Zone*

Wt%	7/16/73	Ru-P18b-73	Ru-P18a-73	Ru-P19-73	Ru-G57-66	Ru-P20-73
SiO_2	37.72	38.25	38.29	39.24	39.76	39.70
Al_2O_3	19.51	19.32	19.84	19.93	19.98	20.27
FeO	11.12	10.12	9.03	7.69	6.99	5.21
MgO	15.17	15.94	16.32	17.92	18.41	19.61
TiO_2	1.66	1.54	1.49	0.43	0.46	1.00
MnO	0.33	0.27	0.35	1.23	0.93	0.41
K_2O	9.29	9.35	9.29	8.93	8.78	8.73
Na_2O	0.30	0.26	0.22	0.26	0.36	0.24
CaO	000	000	000	nd	nd	000
BaO	nd	nd	nd	nd	nd	nd
ZnO	nd	nd	nd	0.02	0.01	nd
H_2O	4.85	.489	5.13	4.34	4.30	4.83

Formula Based on 22 Oxygens

IV	Si	5.502	5.549	5.535	5.569	5.612	5.581
	Al	2.498	2.451	2.465	2.431	2.388	2.419
VI	Al	.855	.852	.914	.902	.935	.941
	Fe	1.356	1.228	1.091	.913	.825	.613
	Mg	3.298	3.447	3.517	3.790	3.873	4.109
	Ti	.182	.168	.162	.131	.099	.106
	Mn	.041	.034	.043	.052	.055	.049
	Zn	–	–	–	.002	.001	–
	Σ	5.732	5.729	5.727	5.790	5.788	5.818
XII	K	1.728	1.730	1.712	1.617	1.580	1.566
	Na	.084	.073	.062	.072	.098	.065
	Ca	000	000	000	–	–	000
	Ba	–	–	–	–	–	–
	Σ	1.812	1.803	1.774	1.689	1.678	1.631

* Data from Guidotti et al (in preparation). Values cited for H_2O by difference from 100 percent. All specimens contain sillimanite.

TABLE 4. Analyses of Biotite from the Lower Sillimanite Zone of the Southeast Portion of the Old Speck Mountain Quadrangle, Maine*

		n16	m49	n23	n18
SiO_2		35.74	36.06	35.87	35.77
Al_2O_3		19.82	19.74	19.75	19.94
FeO		18.59	17.42	16.77	16.94
MgO		10.17	10.83	11.02	11.45
TiO_2		1.81	1.72	1.63	1.44
MnO		0.17	.15	0.19	0.18
K_2O		8.23	8.30	8.48	8.20
Na_2O		0.27	0.28	0.11	0.27
CaO		.002	.000	.008	.000
BaO		nd	nd	nd	nd
ZnO		nd	nd	nd	nd
H_2O		5.11	5.40	6.08	5.71

Formula Based on 22 Oxygens

		n16	m49	n23	n18
IV	Si	5.401	5.433	5.434	5.396
	Al	2.599	2.567	2.566	2.604
VI	Al	.931	.939	.960	.941
	Fe	2.349	2.195	2.124	2.137
	Mg	2.290	2.433	2.488	2.575
	Ti	.206	.195	.185	.164
	Mn	.021	.019	.024	.023
	Zn	–	–	–	–
	Σ	5.797	5.781	5.781	5.840
	K	1.587	1.595	1.639	1.577
	Na	.079	.081	.032	.078
	Ca	.000	.000	.001	.000
	Ba	–	–	–	–
	Σ	1.666	1.676	1.672	1.655

* Data from Cheney (in preparation). Values cited for H_2O by difference from 100 percent. All specimens contain sillimanite.

New Data from Pelitic Schists and Adamellites of Northwestern Maine

Numerous biotites from the pelitic schists of northwestern Maine have been analyzed during the course of petrologic studies by the authors (Guidotti, 1974; Guidotti, Cheney, and Conatore, 1975; and previously unpublished data). These data are presented in Tables 1–5 and were obtained by electron microprobe analysis using the general technique of Bence and Albee (1968). Simple anhydrous silicates and oxides were used as standards. The analytical error is about two percent for elements constituting more than two percent of a given sample.

A rather wide range of biotite Mg/Fe ratios has been found because specimens from pyrrhotite-rich rocks as well as more ordinary pelitic schists have been analyzed. Some of the biotites from the former group of specimens plot well within the phlogopite field of Foster (Fig. 1). All of the biotites from pelitic schists under consideration coexist with minerals such as sillimanite, staurolite, or cordierite. They would plot along the high-Al boundary of the biotite field on an AFM projection, and are clearly Al-saturated for the prevailing P,T conditions. As a result, there is little variation of Al^{VI} or Al^{IV} due to differences in bulk composition. Moreover, because virtually all of the specimens from northwestern Maine have graphite present, one can assume that

TABLE 5. Analyses of Biotites from Two-Mica Adamellites of Northwestern Maine*

Wt%	7-8/3/59	28-8/22/59	12-3/19/59	27-9/10/59	7-8/5/59	25-8/26/59	0-b-41
SiO_2	35.36	35.34	35.62	35.26	35.69	35.87	36.84
Al_2O_3	18.11	19.68	19.64	18.94	18.23	17.76	17.47
FeO	23.59	21.48	20.41	23.18	23.03	23.09	23.69
MgO	6.30	7.50	7.75	6.06	6.73	6.40	6.15
TiO_2	3.16	2.71	3.21	3.45	3.13	3.38	2.26
MnO	.46	.27	.28	.25	.50	.50	1.03
K_2O	9.33	9.27	9.45	9.48	9.50	9.44	9.46
Na_2O	.07	.03	.04	.10	.09	.06	.02
CaO	000	000	000	000	000	000	000
BaO	.10	.05	.07	.07	.12	.07	.06
ZnO	.04	.04	.02	.05	.03	.02	.08
H_2O	3.42	3.56	3.44	3.11	3.06	3.37	2.91

Formula Based on 22 Oxygens

		7-8/3/59	28-8/22/59	12-3/19/59	27-9/10/59	7-8/5/59	25-8/26/59	0-b-41
IV	Si	5.438	5.366	5.377	5.387	5.449	5.496	5.632
	Al	2.562	2.634	2.623	2.613	2.551	2.504	2.368
VI	Al	.720	.888	.871	.797	.730	.704	.780
	Fe	3.034	2.728	2.577	2.962	2.940	2.958	3.029
	Mg	1.443	1.698	1.745	1.381	1.531	1.461	1.401
	Ti	.366	.309	.364	.396	.359	.389	.259
	Mn	.060	.035	.036	.032	.043	.064	.134
	Zn	.005	.005	.002	.006	.004	.003	.008
	Σ	5.628	5.663	5.595	5.574	5.607	5.579	5.611
XII	K	1.831	1.796	1.819	1.847	1.850	1.846	1.844
	Na	.021	.009	.013	.031	.026	.017	.004
	Ca	000	000	000	000	000	000	000
	Ba	.006	.003	.004	.005	.007	.004	.003
	Σ	1.858	1.808	1.836	1.883	1.883	1.867	1.851

* Specimens (28-), (12-), and (27-) contain sillimanite. Value cited for H_2O by difference from 100 percent.

Fe^{3+} is probably present in low and uniform amounts. The above considerations will now enable us to make a concise evaluation of any relationship between Al^{VI} and the $Mg/(Fe^{2+} + Mn)$ ratio.

Figure 2 shows the relative amounts of $(Fe^{2+} + Mn)$, Mg, and Al in the octahedral sheets of biotites from pelitic schists of northwestern Maine. Also shown are analyses of biotites from several igneous parageneses. With respect to the biotites from pelitic schists, it is evident that no marked relationship exists between Al^{VI} and the $Mg/(Fe^{2+} + Mn)$ ratio. Biotites A, B, and C come from *sillimanite-bearing* adamellites which intrude the pelitic schists of northwestern Maine. Hence, they can be legitimately compared with the biotites discussed above and thereby extend the range of Mg/Fe ratios to still lower values (to 0.466).

Biotites D, E, F, and G are from adamellites which contain no sillimanite. The absence of sillimanite suggests a lower activity for Al_2O_3 in these specimens. Of note is the fact that on Figure 2 these biotites plot at lower Al values than do biotites A, B, and C.

Figure 3 is similar to Figure 2, but includes Ti^{4+} in with R^{3+}. Comparison of the trends on the two diagrams shows that in Figure 3 there is a distinct suggestion of a decrease of R^{3+} as Mg increases. Moreover, our data do show that Ti^{4+} decreases as Mg increases in biotite (see Tables 1–5) and that this inverse trend must be controlled by crystallochemical factors, because all specimens coexist with a Ti-saturating phase[2] (rutile in the pyrrhotite-rich specimens and ilmenite in the others).

It is thus clear that at least part of the trend shown on Figure 1 can be explained by inclusion of Ti^{4+} with R^{3+}. The remainder of the trend can be attributed to inclusion of Fe^{3+} in R^{3+} and to the availability of samples as exemplified by previous analyses of low-Al phlogopites only from marbles,

calc-silicates, and ultramafic rocks. Moreover, our use of biotites from only a few similar parageneses has greatly reduced the amount of scatter in terms of the $R^{3+}/(Mg + Fe^{2+} + Mn)$ ratio on both Figure 2 and Figure 3 relative to that seen on Figure 1.

Conclusions

(1) The present data demonstrate no clear relation between $Mg/(Fe^{2+} + Mn)$ and Al^{VI} content of biotite over most of the biotite composition range. However, our data do not preclude such a relationship in biotites approaching the annite-siderophyllite join. For those compositions, structural arguments suggest that a pure Fe octahedral sheet may not be stable (Hazen and Wones, 1972).

(2) Our data demonstrate the dangers of trying to infer crystallochemical relationships in rock-forming solid solutions using data based on specimens from many different parageneses.

References

Bence, A. E., and A. L. Albee (1968) Empirical correction factors for the electron microanalysis of silicates and oxides. *J. Geol.* **76**, 382–403.

Foster, M. D. (1960) Interpretation of the composition of trioctahedral micas. *U. S. Geol. Surv. Prof. Pap.* **354-B**, 11–46.

Gower, J. A. (1957) X-ray measurements of the iron-magnesium ratio in biotites. *Am. J. Sci.* **255**, 142–156.

Guidotti, C. V. (1974) Transition from staurolite to sillimanite zone, Rangeley Quadrangle, Maine. *Geol. Soc. Am. Bull.* **85**, 475–490.

———, J. T. Cheney, and P. D. Conatore (1975) Coexisting cordierite + biotite + chlorite from the Rumford Quadrangle, Maine. *Geology*, **3**, 147–148.

Hazen, R. M., and D. R. Wones (1972) The effects of cation sub-sittutions on the physical properties of trioctahedral micas. *Am. Mineral.* **57**, 103–129.

[2] Foster (1960, p. 26) also noted that Ti was low in phlogopites, but gave no mention of the presence or absence of a Ti-saturating phase.